7

Use of Rapid Prototyping and 3D Reconstruction in Veterinary Medicine

Elisângela Perez de Freitas[1], Pedro Yoshito Noritomi[2] and Jorge Vicente Lopes da Silva[2]
[1]*Department of Veterinary Surgery and Anesthesiology, College of Veterinary Medicine and Animal Science – São Paulo State University (UNESP)*
[2]*Tridimensional Technologies Division, Renato Archer Information Technology Center (CTI)*
Brazil

1. Introduction

1.1 Medical image processing

In veterinary medicine, as well as in medicine, many noninvasive image techniques have been used for pathology diagnosis. The most oftenly used methods are computed tomography (CT) and magnetic resonance imaging (MRI) (Lim & Zein, 2006). In general, these equipments generate a sequence of 2D images which make it difficult to display the spatial relationship of the important structures (Qiu et al., 2004). The 2D images are digitally stored in the international standard DICOM (Digital Imaging and Communications in Medicine) file format simplifying the interoperability among different medical systems with no extra costs for data conversion. This file format contains the necessary data for three-dimensional (3D) reconstruction and patient information. Specifically developed reconstruction software, based on these 2D DICOM files, can generate the correspondent 3D models of the region of interest. By means of the software, internal and external anatomy can be clearly shown, measured, highlighted, and segmented either simultaneously or separately.

1.2 Rapid prototyping

Rapid prototyping is an additive process based on a computer controlled deposition of layers of materials. It was first available a little more than two decades ago, to speed up and facilitate solutions in automobile and aeronautical product development. In a few years it started to be used in the medical field, for reconstructive surgery, helping surgeons with a perfect replica of the anatomy of the patient. Nowadays, rapid prototyping is also known as additive manufacturing and is widespread in many areas of knowledge.

A virtual model is electronically sliced and sent to the machine that deposits each layer at a time. In the process to build a physical model from a virtual one many different processes are present using polymeric materials in different forms such as liquids,

powders, sheets, and filaments. Other materials such as metals, ceramics, and paper can also be used. To glue each layer on top of the other there are processes based on lasers, binders, extrusion, etc.

The advantage of RP technologies is their ability to produce complex 3D physical models from a three-dimensional computer model (Geng et al., 2005). The main processes of rapid prototyping are: Selective Laser Sintering (SLS) based on the melting of a fine polymeric powder by means of heating lasers; Estereolitography (SLA) that is based on the polymerization of a liquid resin by means of specific wavelength lasers; Fused Deposition Modeling (FDM) where a filament is extruded and deposited continuously in thin threads of polymeric materials; and Tridimensional Printing (3DP) where each layer of powder is glued to the upper by means of ink jetting a binder. There are available today about thirty commercial processes including the above and its variations.

2. Veterinary clinical cases

2.1 Dogs: 3D model of different type of dog's skull

Dogs are categorized as dolichocephalic (Doberman, Collie, Setter, Whippet), mesaticephalic (Rottweiler, Poodle, Cocker spaniel) and brachycephalic (Boxer, Bulldog, Pug). The mandibular structure can be different according to the type of dog's skull. This mandibular structure may vary in three ways: on the cortical bone's width of the mandibular body, mandibular size in relation to the maxilla or the type of dental occlusion in these animals. It is really important that the surgeon is knowledgeable about the specifics of each kind of dog, in order for him to choose the best surgical technique for the mandible fracture or orthognathic corrections, then to re-habilitate occlusion and masticatory function, to make them the closest to normal function as possible. This study has the goal to offer mandibular images in a normal pattern of Doberman, Rottweiler, Poodle and Boxer so that they can help as comparison tools between normal or affected structures. The animals were anesthetized and physical examination indicated no abnormalities in the mandible. Sequential transverse images of each dog's head were acquired on a helical CT Scanner (Shimadzu SCT-7800CT). The data obtained was saved in DICOM file format. 3D reconstructed images of the mandible were made by software programs commercially available. The virtual models were used to perform the measurements of length, height and width of the mandible and measurements of the cortical bone of the mandible body. The results are described in Table 1 and Figure 1, 2.

Dog breed	Cortical bone (mm)	Length (mm)	Height (mm)	Width (mm)
Doberman	4,3	185,8	28,3	11,8
Rottweiler	5,2	162,8	27,2	19,5
Poodle	2,7	77,0	10,2	7,9
Boxer	4,7	137,7	20,8	11,6

Table 1. Measurements of the mandible for the different dog breeds.

This study has the goal to build the 3D reconstructed model of the mandible in a normal pattern of Doberman, Rottweiler, Poodle and Boxer so that they can help as comparison tools between normal and affected structures.

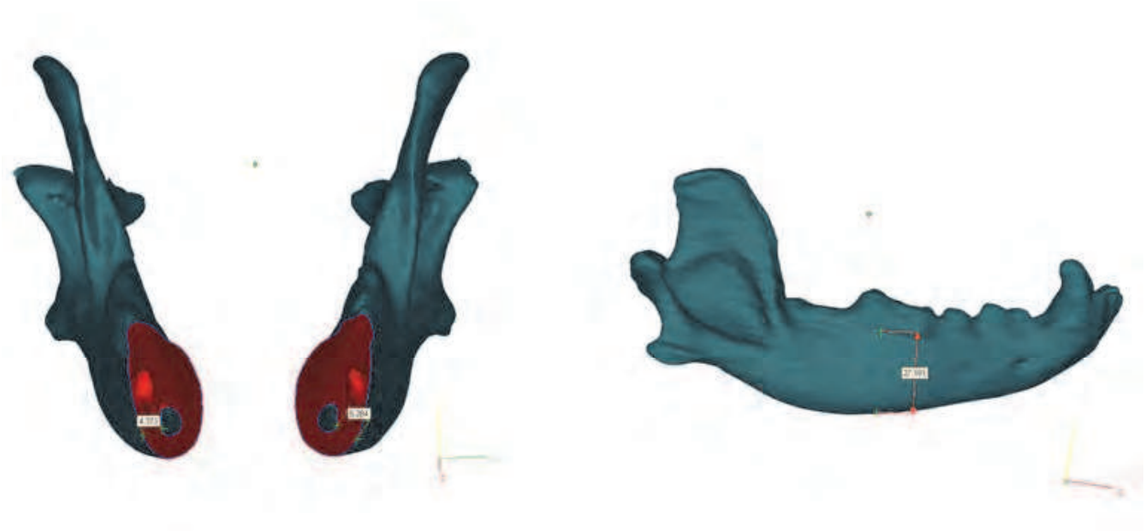

Fig. 1. Measurements of the cortical bone and height of the Rottweiler's mandible.

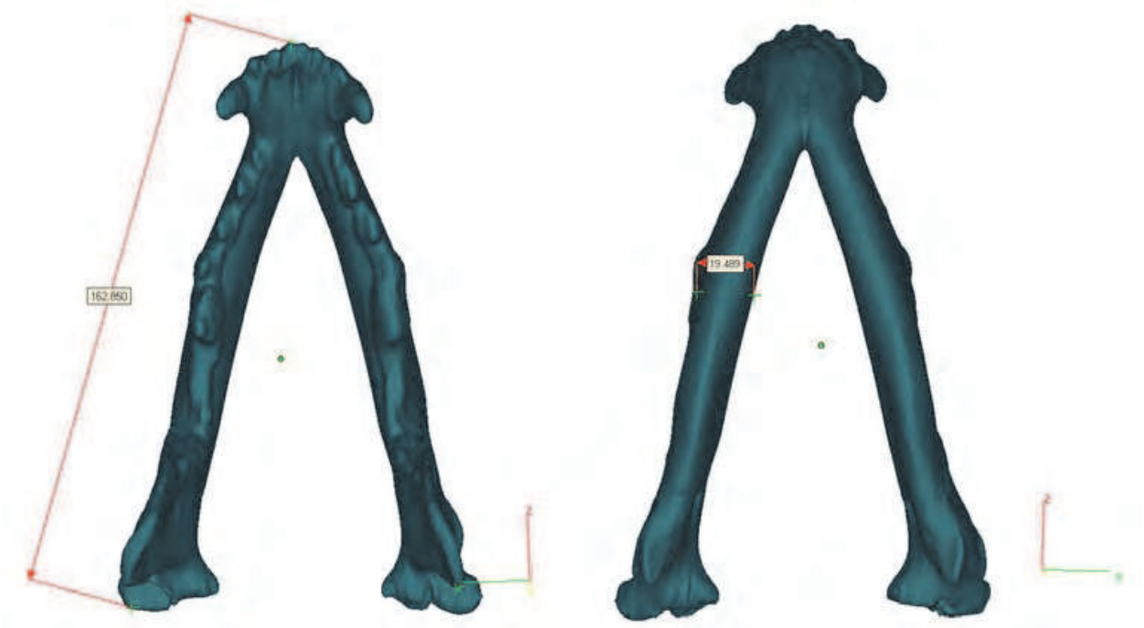

Fig. 2. Measurements of the length and width of the Rottweiler's mandible.

2.2 Fox: orthopedic treatment of the maxillofacial malformation

A fox (*Pseudalopex vetulus)*, 9-month-old free-ranging, 3.7 kg male was presented to the Veterinary Hospital with Class II malocclusion – posterior cross-bite – on the right side (Freitas et al., 2010a). The animal was anesthetized and oral examination revealed the right

mandibular canine tooth distal to the right maxillary canine tooth and tipped in a buccal direction. Because of this, the left mandibular canine caused a lesion on the palate between the left maxillary 3rd incisor and canine teeth. Sequential transverse images of the head were acquired on a helical CT Scanner (Shimadzu SCT-7800CT) with the fox placed in dorsal recumbency. The InVesalius software was also used to edit and measure the original 3D virtual model obtained directly from the CT scan, and the Magics X SP2 was used to generate the final model for the prototype machine. The virtual 3D model of the head showed facial and mandibular asymmetry (Figure 3). The physical prototype constructed by the 3DP (Z-Cortp) technique enabled the preoperative planning (Figure 4 and 5). The inclined plane technique was used to correct crossbite and avoid palate injury. The fox adapted well to the treatment showing signs of discomfort only in the first 48 h. The inclined plane was removed after three months and a new CT exam was performed. Visualization of 3D images in combination with rapid prototyping allowed the surgeon to perform 3 sets of geometric measurements in the virtual model on the first and second examination. Comparison of the prototypes and oral examination confirmed less maxillofacial discrepancy. Furthermore, the palate injury healed because the left mandibular canine tooth was not making contact with the palatal tissues. This orthopedic treatment showed that the Plana's technique has satisfactory results while modifying the skeletal structure stimulating the development of the stomatognatic system. In this case, the visualization and segmentation of CT images and 3D reconstruction of skull aided the surgical planning. The comparison of the prototype before and after treatment allowed a qualitative improvement of the occlusion.

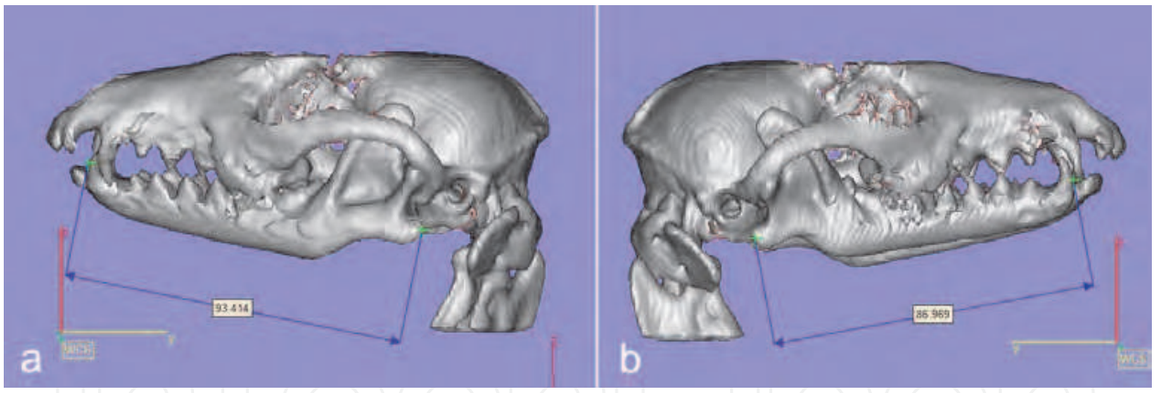

Fig. 3. Virtual 3D model (Magics X SP2) of the head based on CT image data showing the left mandible (a) is bigger than the right mandible (b).

2.3 Rabbit: 3D finite element analysis

The finite element analysis (FEA) is one of the most promising tools in the study of functional morphology of the craniofacial skeleton in humans and other species (Richmond et al., 2005). It is a computationally intensive engineering technique that estimates how objects of complex design resist loads (Wang et al., 2006). CT imaging is a useful method to gather three-dimensional physiological data such as bone geometry and density *in vivo* (Keyak et al., 1990). The results of von Mises' stress distribution in a human model of normal mandible showed that the model was reliable (Vollmer et al., 2000). Despite advances in commercially available meshing programs for creating subject-specific models

Fig. 4. Photograph of the prototype of the fox's skull.

Fig. 5. Photography showing dorsal (a) and ventral (b) view of the prototype. Note the mandibular asymmetry.

from image data, the process is still expensive, in terms of time, and usually requires high level of user intervention (Wilcox, 2007). In this study, three-dimensional (3D) geometrical and finite element analysis (FEA) of the mandible of a rabbit were built in order to evaluate the distribution of stresses on mandible of the rabbit applying a masticatory force of 10 Newtons (N).

A computerized tomography (CT) examination was performed on the head of the Norfolk rabbit, female, 2 months of age. In order to perform CT studies the animal was submitted to general anesthesia. Sequential transverse images of the head were acquired on a helical scanner (Shimadzu SCT-7800CT) with the rabbit placed in a dorsal recumbency. The scanning parameters were 120kVp, 170 mA, 1.0 mm slice thickness, 1.0mm interval, pitch of 2.0, and 1 s/rotation (Figure 6). A virtual 3D model of the head was generated based on CT image data, in DICOM (Figure 7). The 3D model was saved in STL format and it was prototyped (Figure 8). The STL model was imported into the software Rhinoceros® in order to create the BioCAD representation of the mandible prototype of the head was created. The BioCAD was used as a reference to create a more complex 3D model, demanded by the finite element analysis. The complete CAD models were exported to the NEiNastran®, finite elements analysis program, using IGES file format. The finite elements analysis was performed by using a tetrahedral elements mesh (Figure 9). Isotropic, linear and homogeneous material properties were assumed for the bone. The study of total translation distribution on mandible and opposite action of the masseter muscle had to be made by NEiNastran® (Figure 10). The masticatory forces of the 10 N were applied on mandible in order to simulate a typical rabbit bite.

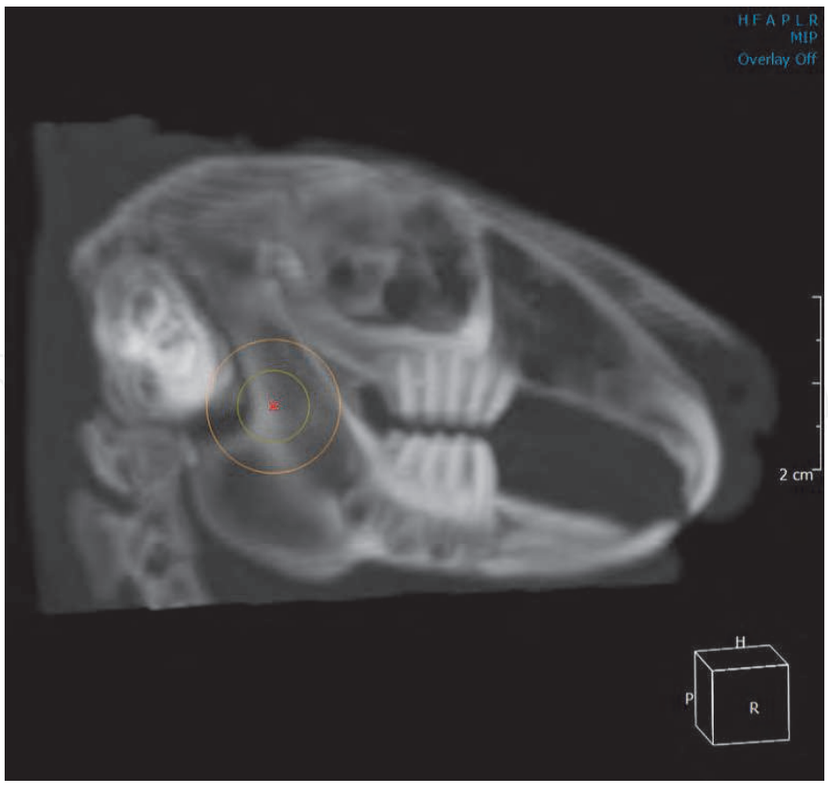

Fig. 6. Image showing the reconstruction of the rabbit's head.

Fig. 7. Image of the 3D virtual model of the rabbit's skull.

Fig. 8. Photography of the rabbit skull prototype.

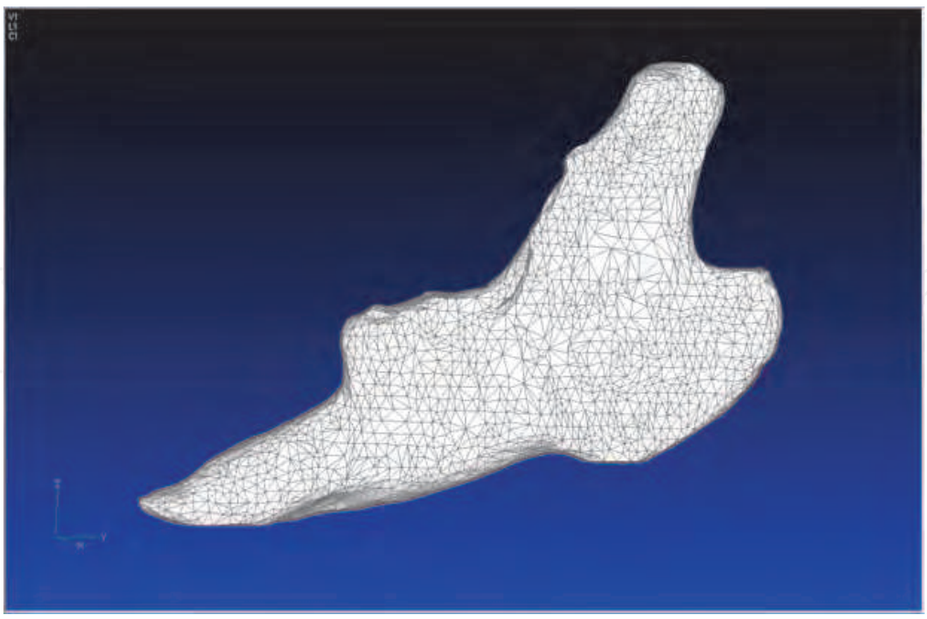

Fig. 9. Finite element mesh on the rabbit's mandible.

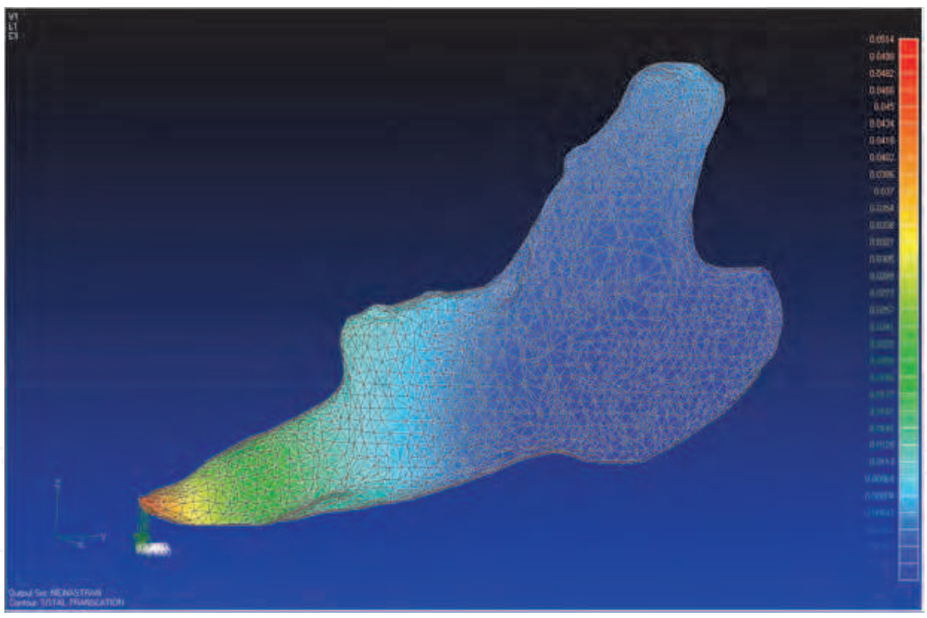

Fig. 10. Total translation distribution on the rabbit's mandible.

The FEA has show von Mises' stress concentration for the rabbit's mandible. There was a major von Mises' stress concentration on the cranial region of the mandible (Figure 11), with compressive stress propagation on the ventral side of the mandibular canal, with a tractive stress on the dorsal side of the same mandibular canal, on the third middle of the mandibular body. Both, the compressive and tractive stress fields follow through the mandibular body, drawing a stress triangle with the vertical ramus of the mandible on retro-molar region.

Previous studies have reported that the distribution of von Mises' stresses on the human normal mandible occurred on the posterior coronoid process, mandibular angle and distal alveolar ridge in the molar area (Tie et al., 2006). In another hand, in this study with rabbit, the von Mises' stress concentration occurred on the cranial region of the mandible. Both the compressive stress and tractive stress distribution occurred through the mandibular body of the rabbit, drawing a stress triangle with the vertical ramus of the mandible on retro-molar region. Analyzing von Mises' stress concentration for normal mandible, it was important because the stress distribution has a great effect on biomechanical properties of reconstructed mandibles. If stress distribution is too concentrated, the bone will not regenerate but will be absorbed (Song & Xue, 1999).

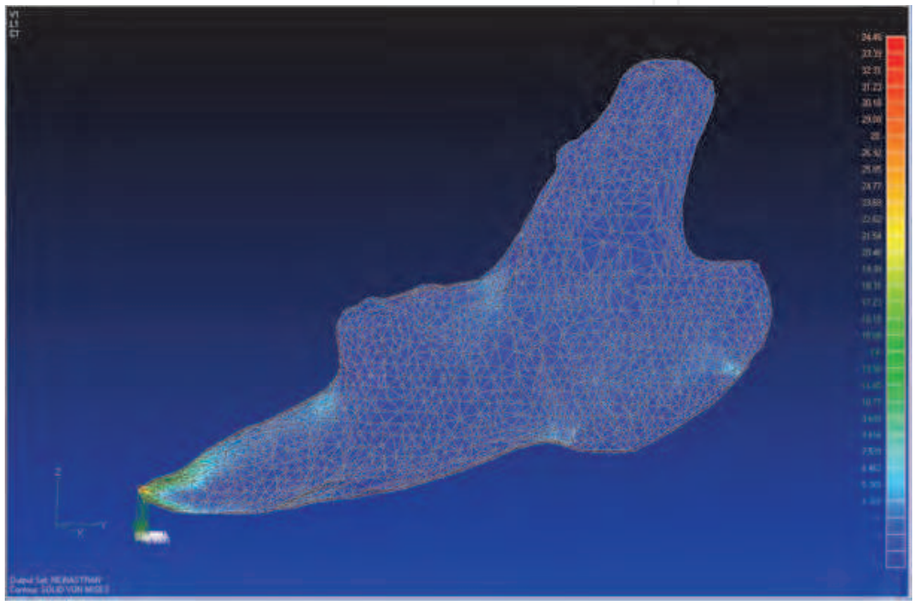

Fig. 11. Rostral area of the rabbit mandible showing a maximum von Mises' stresses.

2.4 Dog: bone plate for mandibular fracture

The present study aimed to develop a plate for treating oblique fractures of the mandibular body in dogs and to validate the project by using finite elements and biomechanical essays from the prototype of the mandible (Figure 12).

A computerized tomography (CT) examination was performed on the head. The obtained 3D virtual model was used as reference to develop the plate and the monocortical screws. The prototypes were used as samples for the mechanical evaluations. The same head utilized for the CT scan was used to perform the surgical procedure. The dog's head was positioned in left lateral recumbency, and the right mandible area was clipped, prepared, and draped using a sterile technique. A longitudinal skin incision was performed to the ventral midline of the right mandible from the level of the third molar tooth to the level of the fourth lower right premolar tooth. The subcutaneous fascia, and platysma and digastric muscles were incised and retracted to expose the vestibular face of the mandible. An oblique ventrorostral fracture was induced between the second and the first lower right molar using a gig saw. Then, fracture reduction and osteosynthesis were performed using titanium screws and a plate, the same procedure as in the prototype (Figure 13).

Fig. 12. Prototype of the mandible.

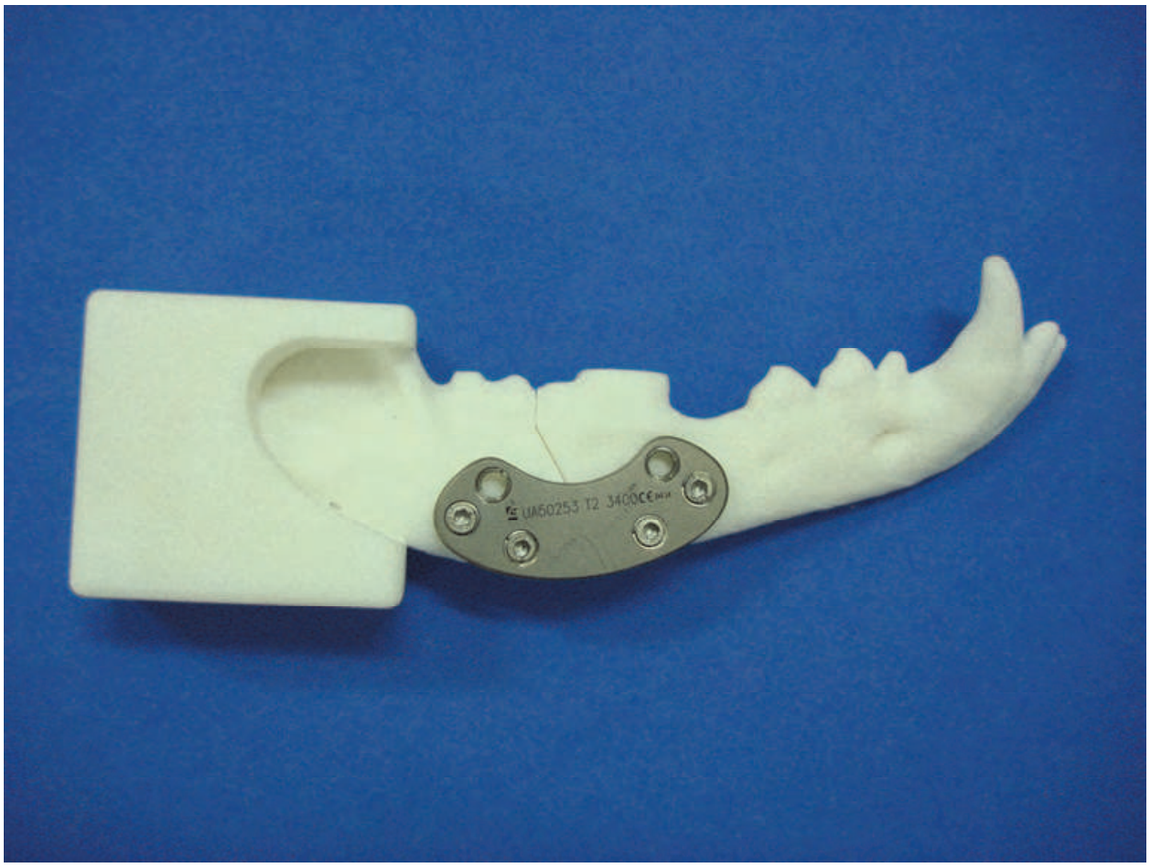

Fig. 13. Prototype of the mandible with plate and screws.

Two screws were placed at each end of the fracture, since the mechanical tests had shown this to be a satisfactory system for this type of fracture. The elevated muscles were sutured to the fascia on the surface mandible using a simple continuous pattern, and the skin incision closed using simple interrupted pattern. Nylon monofilament 4-0 was the suture material used for all tissue layers. Another CT scan was performed to observe the placement of screws (Figure 14).

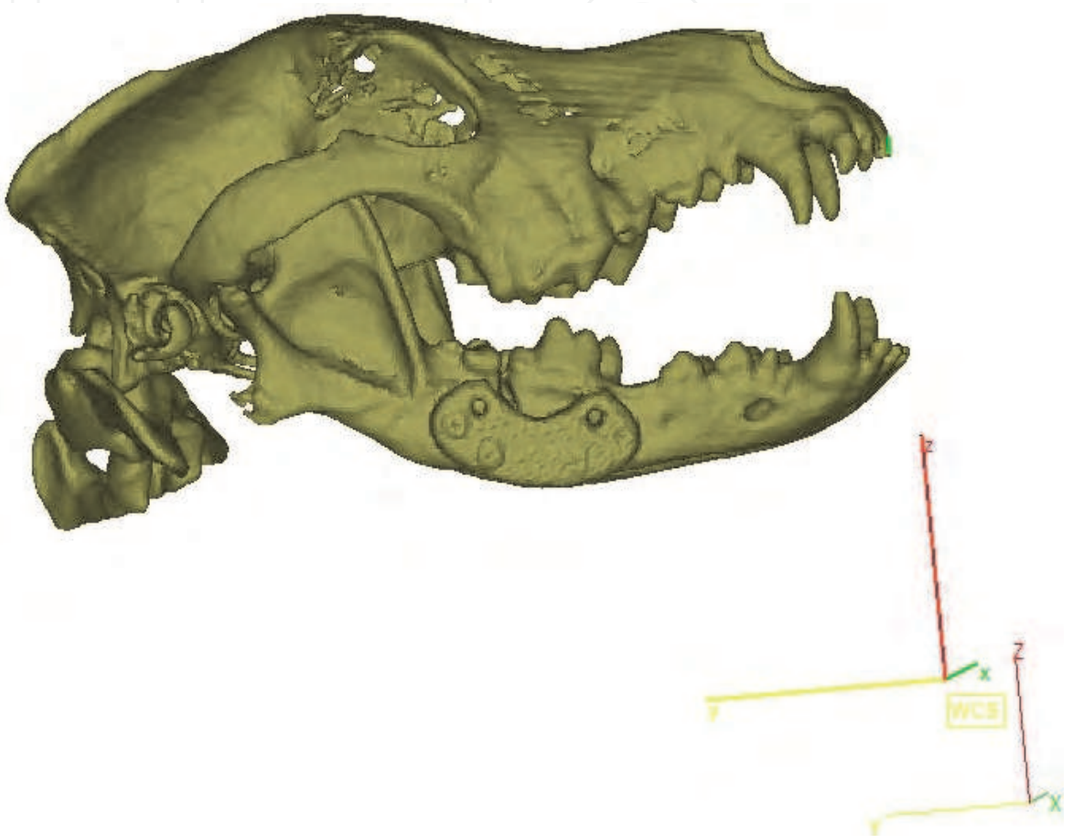

Fig. 14. 3D virtual model of the dog head with plate and screws.

The bone plate developed in the present experiment achieved proper mechanical resistance as proven by mechanical tests and finite element studies. Furthermore, its positioning next to the alveolar surface of the mandible bone, considered the site of maximum tension stress (Freitas et al., 2010b), as well as its design and thickness, render it better for application. In addition, the stabilization of the bone plate using blocked monocortical screws avoided the damage to dental roots and neurovascular structures that was observed in CT studies. In the SPS Free-Block system the screw is blocked due to the presence of a lock ring positioned inside the plate hole. Besides, this lock ring allows the screw be positioned at different angles. The guidelines adopted during the development of implants and the validation tests used will be discussed.

The mandible bone has a thick cortex and high mechanical resistance (Ashman et al., 1985). Because of this the cortical bone tends to behave as an isotropic material (Ashman et al., 1985; O'Mahony et al., 2000). The materials used to produce the prototypes and the system of plates and screws, nylon 6 and titanium, respectively, are also considered isotropic,

linear, homogeneous and elastic materials. However, in order to establish the mechanical properties of the sintered nylon 6, traction tests were performed on rectangular specimens. This test enabled the establishment of the elasticity module and Poisson coefficient (Anusavice, 2005), both necessary to perform the finite element analysis. The mechanical test performed in the prototype showed the resistance difference between the fracture types. The maximum force to reach the plastic phase, when the material lost its original properties, was four times higher for favorable than for unfavorable fracture (Freitas et. al, 2010b). Unfavorable fracture tends toward dorsal distraction of the caudal fractured segment and ventral displacement of the cranial fractured segment (Harvey & Emily, 1993; Wiggs & Lobprise, 1997; Hall & Wiggs, 2005). Due to these results and high cost of the prototypes, a force of 40N was established to perform the tests. This force is within the range of elastic deformation for the fracture with less resistance. Since the prototypes maintained their initial properties, the tests were considered valid.

The results of the flexile tests performed in favorable and unfavorable fracture prototypes showed that the greater the number of screws used for stabilization of the bone plate, the higher the relative rigidity of the system, and the smaller the deflection. However, comparing both fracture types, the relative rigidity values of the favorable fracture were approximately two times those of the unfavorable fracture. These findings suggest that not only the number of screws used, but also the fracture type, had significant influence on plate fixation.

On the other hand, comparing these findings with the finite element data, it can be observed that the principal maximum stress for favorable fractures displayed an unexpected behavior. Based on the number of screws removed there was better stress distribution in the bone, with a decrease of principal maximum stress value from 20.60 MPa to 15.34 MPa (Freitas et al, 2010b).

The stress distribution has significant influence on biomechanical properties of surgically reconstructed mandible; if concentration of stress distribution occurs the bone will be reabsorbed instead of being regenerated (Tie et al., 2006).

Both von Mises' stress and force transmission showed that in a favorable fracture based on screw removal there was higher stress concentration on the lower screw positioned in the cranial fractured segment. Probably this is associated with the positioning of this screw in the direction of the load application. On the other hand, in the unfavorable fracture the von Mises' stress was higher in the lower screw positioned in the caudal fractured segment, suggesting that the bone plate probably supports and rotates around this screw. Since this type of fracture does not offer support to cranial fractured segment by means of the caudal fractured segment, the stress distribution was concentrated in the ventral part of the bone plate that suffered constant traction during load application. Since the caudal fractured segment tends to dorsal displacement due to the muscular pull and the caudal fractured segment does not offer resistance, only the plate was able to maintain the stability in this fracture type.

In conclusion, the double-arch geometry plate fixed with blocked monocortical screws presents sufficient resistance to stabilize oblique fractures of the mandibular body, without compromising the dental or neurovascular structures.

2.5 Bird: orthosis produced by rapid prototyping

A Brazilian bird of prey called southern caracará (*C. plancus*) adult was found in wild life and brought to the veterinary hospital with a thin thread constricting its posterior left

member. The clinical examination showed necrosis in the tibiotarsal joint. The patient was submitted to general anesthesia to perform amputation of the member. After surgery the bird presented difficulties in to adaptating to the captive environment, specially concerning to locomotion and standing.

In order to improve the bird´s quality of life an orthosis was specially designed using the concepts of the paralympic runner Oscar Pistorius. Using the information of a CT acquisition of the contralateral healthy member and mirroring the data the perfect shape and dimensions were obtained. The information was used to design an optimized fitting orthosis that was later produced directly by means of the SLS rapid prototyping technique (Figure 15). The internal region that should be in contact with the animal´s skin was covered by a layer of dentistry addition silicone to avoid injury in the area (Figure 16).

The final result showed a difficulty of the animal to adapt with the osthosis and after some hours it was taken out (Figure 17). The same process was repeated for three days and at the end the animal presented a trauma on the skin, having tried to release it with its beak (Figure 18). Unfortunately the animal did not adapt to the orthosis and further studies have to be developed for successful adaptation.

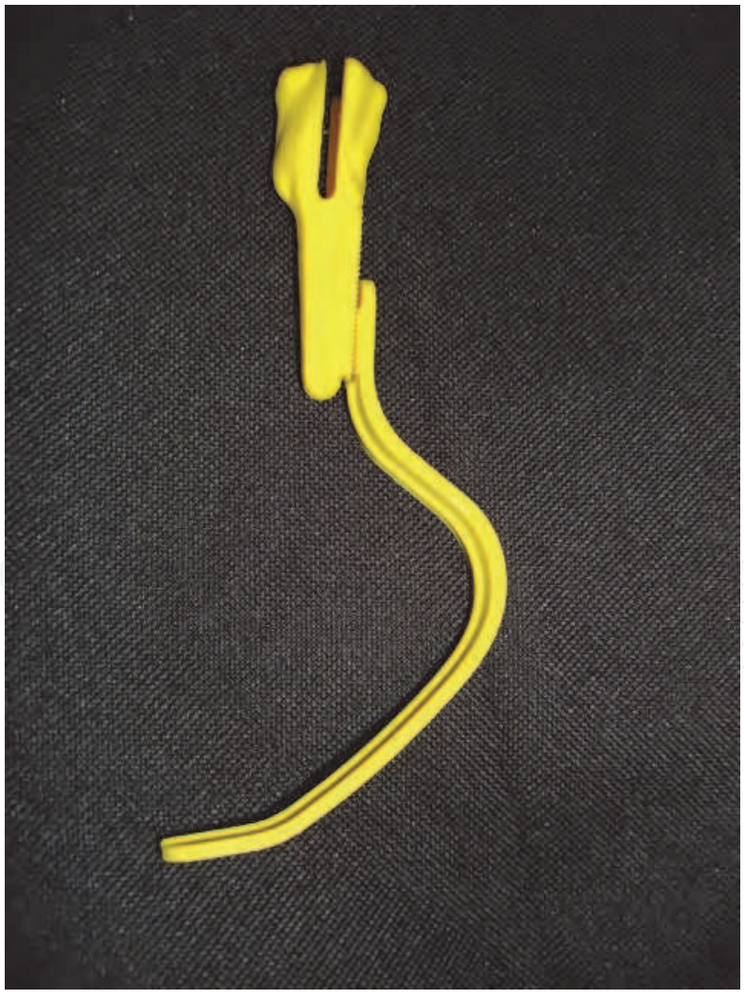

Fig. 15. Orthosis produced by means of the SLS rapid prototyping technique.

Fig. 16. Southern Caracará with orthosis on the posterior left member.

Fig. 17. Southern Caracará trying to release the member with beak.

Fig. 18. Injury on the skin of the Caracará.

3. Conclusions

3D medical models and rapid prototyping opened up new possibilities for the surgical planning and treatment of wild and domestic animals, allowing for anatomy studying and to support diagnosis in order to minimize the anesthetic period during surgery. It can be a good opportunity to increase the welfare of some rare animals or of the ones considered to be in danger of extinction. In this situation these animals can even have a better reproduction.

4. Acknowledgements

The authors are grateful to the professionals of Tridimensional Technologies Division of Renato Archer Information Technology Center – CTI.

5. References

Anusavice, K.J. (2005). *Phillips materiais dentários,* 11ed, Elsevier, ISBN 85-352-1532-8, Rio de Janeiro.

Ashman, R.B.; Rosinia, G.; Cowin, S.C.; Fontenot, M.G. & Rice, J.C. (1985). The bone tissue of the canine mandible is elastically isotropic, *Journal of Biomechanics*, 18, (1985), 717-721, ISSN 0021-9290.

Freitas, E.P.; Rahal, S.C.; Teixeira, C.R.; Silva, J.V.L.; Noritomi, P.Y.; Villela, C.H.S.; Yamashita, S. (2010a). Rapid prototyping and inclined plane technique in the

treatment of maxillofacial malformations in a fox, *Canadian Veterinary Journal,* 51 (March 2005), 267-270, ISSN 0008-5286.

Freitas, E.P.; Rahal, S.C.; Gioso, M.A.; Vulcano, L.C.; Shimano, A.C.; Silva, J.V.L.; Noritomi, P.Y. & Warrak, A.O.E. (2010b). Finite element modeling for development and optimization of a bone plate for mandibular fracture in dogs, *Journal of Veterinary Dentistry,* 27, 4 (December 2010), 212-221, ISSN 0898-7564.

Geng, L.; Feng, W.; Hutmacher, D.W.; Wong, Y.S.; Loh, H.T. & Fuh, J.Y.H. (2005). Direct writing of chitosan scaffolds using a robotic system, *Rapid Prototyping Journal,* 11, 2, (2005), 90-97, ISSN 1355-2546.

Hall, B.P. & Wiggs, R.B. (2005). Acrylic splint and circumferential mandibular wire for mandibular fracture repair in a dog, *Journal of Veterinary Dentistry,* 22, 3, (September 2005), 170-175, ISSN 0898-7564.

Harvey, C.E.; Emily, P.P. (1993). *Small animal dentistry*, Mosby, St. Louis.

Keyak, J.H.; Meagher, J.M.; Skinner, H.B. & Mote, Jr. C.D. (1990). Automated three-dimensional finite element modeling of bone: a new method, *Journal of Biomedical Engineering,* 12, 5, (September 1990), 389-397, ISSN 0141-5425.

Lim, J.; Zein, R. (2006). The digital imaging and communications in medicine (DICOM): description, structure and applications, In: *Rapid Prototyping – Theory and Practice,* Kamrani, A. & Nasr, E.A. (Ed.), 63-86, Springer, ISBN-13 9780387232904, New York.

O'Mahony, A.M.; Williams, J.L.; Katz, J.O. & Spencer, P. (2000). Anisotropic elastic properties of cancellous bone from a human edentulous mandible, *Clinical Oral Implants Research,* 11, (2000), 415-21, ISSN 0905-7161.

Qiu, M.G.; Zhang, S.X.; Liu, Z.J.; Tan, L.W.; Wang, Y.S.; Deng, J.H. & Tang, Z.S. (2004). Three-dimensional computational reconstruction of lateral skull base with plastinated slices, *The Anatomical Record Part A,* 278, A, (2004), 437-442, ISSN 1552-4892.

Richmond, B.G.; Wright, B.; Grosse, I.; Dechow, P.C.; Ross, C.F.; Spencer, M.A. & Strait, D.S. (2005). Finite element analysis in functional morphology, *Anatomical Record,* 283, A, (March 2005), 259-274, ISSN 0003-276X.

Song, G. & Xue, M. (1999). Stress-adaptation of bone, *Journal of Biomedical Engineering,* 16, 4 (December 1999), 502-505, ISSN 0141-5425.

Tie, Y.; Wang, D.M.; Ji, T., Wang, C.T. & Zhang, C.P. (2006). Three-dimensional finite-element analysis investigating the biomechanical effects of human mandibular reconstruction with autogenous bone grafts, *Journal of Cranio-maxillofacial Surgery,* 34, 5, (July 2006), 290-298, ISSN 1010-5182.

Vollmer, D.; Meyer, U & Joos, D. (2000). Experimental and finite element study of a human mandible, *Journal of Cranio-maxillofacial Surgery,* 28 (April 2000), 91-96, ISSN 1010-5182.

Wang, Q.; Strait, D.S. & Dechow, P.C. (2006). A comparison of cortical elastic properties in the craniofacial skeletons of three primate species and its relevance to the study of human evolution, *Journal of Human Evolution,* 51, 4, (October 2006), 375-382, ISSN 0047-2484.

Wiggs, R.B. & Lobprise, H.B. (1997). *Veterinary Dentistry: principles and practice,* Lippincott-Raven, Philadelphia.

Wilcox, R.K. (2007). The influence of material property and morphological parameters on specimen-specific finite element models of porcine vertebral bodies. *Journal of Biomechanics*, 40, 3 (2007), 669-673, ISSN 0021-9290.

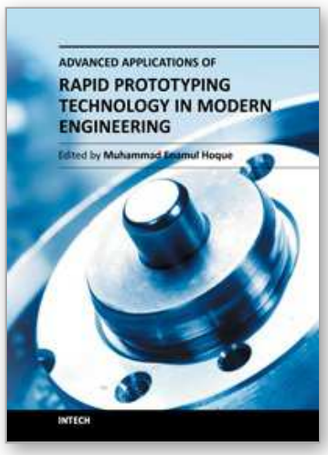

Advanced Applications of Rapid Prototyping Technology in Modern Engineering

Edited by Dr. M. Hoque

ISBN 978-953-307-698-0
Hard cover, 364 pages
Publisher InTech
Published online 22, September, 2011
Published in print edition September, 2011

Rapid prototyping (RP) technology has been widely known and appreciated due to its flexible and customized manufacturing capabilities. The widely studied RP techniques include stereolithography apparatus (SLA), selective laser sintering (SLS), three-dimensional printing (3DP), fused deposition modeling (FDM), 3D plotting, solid ground curing (SGC), multiphase jet solidification (MJS), laminated object manufacturing (LOM). Different techniques are associated with different materials and/or processing principles and thus are devoted to specific applications. RP technology has no longer been only for prototype building rather has been extended for real industrial manufacturing solutions. Today, the RP technology has contributed to almost all engineering areas that include mechanical, materials, industrial, aerospace, electrical and most recently biomedical engineering. This book aims to present the advanced development of RP technologies in various engineering areas as the solutions to the real world engineering problems.

InTech Europe
University Campus STeP Ri
Slavka Krautzeka 83/A
51000 Rijeka, Croatia
Phone: +385 (51) 770 447
Fax: +385 (51) 686 166
www.intechopen.com

InTech China
Unit 405, Office Block, Hotel Equatorial Shanghai
No.65, Yan An Road (West), Shanghai, 200040, China
中国上海市延安西路65号上海国际贵都大饭店办公楼405单元
Phone: +86-21-62489820
Fax: +86-21-62489821

IntechOpen